AGU PUBLICATIONS

Geophysical Research Letters

RESEARCH LETTER
10.1002/2014GL062204

Key Points:
- IS is sensitive to collisions when the mean free path is close to the wave number
- Multifrequency measurements allow for direct inference of collision frequency
- Can be used to investigate neutral atmosphere and collision models

Correspondence to:
M. J. Nicolls,
michael.nicolls@sri.com

Citation:
Nicolls, M. J., H. Bahcivan, I. Häggström, and M. Rietveld (2014), Direct measurement of lower thermospheric neutral density using multifrequency incoherent scattering, *Geophys. Res. Lett.*, *41*, 8147–8154, doi:10.1002/2014GL062204.

Received 13 OCT 2014
Accepted 3 NOV 2014
Accepted article online 6 NOV 2014
Published online 1 DEC 2014

Direct measurement of lower thermospheric neutral density using multifrequency incoherent scattering

Michael J. Nicolls[1], Hasan Bahcivan[1], Ingemar Häggström[2], and Michael Rietveld[3]

[1]Center for Geospace Studies, SRI International, Menlo Park, California, USA, [2]EISCAT Scientific Association, Kiruna, Sweden, [3]EISCAT Scientific Association, Ramfjordmoen, Norway

Abstract Incoherent scatter (IS) is sensitive to collisional properties of the ion gas when the mean free path is close to the radar wave number. However, it has been traditionally difficult to infer the rate of collisions from IS measurements because of ambiguities in the theory for measurements at a single wave number (k). We demonstrate that multifrequency measurements to achieve diversity in k can allow for direct inference of the composition-weighted ion-neutral collision frequency in the upper mesosphere and lower thermosphere. By direct, we mean that no significant constraints are imposed on the interpretation of the IS spectra and that interpretation relies only on the IS formalism (rather than a steady state ion-momentum equation, for example). The technique is demonstrated using measurements from the European Incoherent Scatter VHF and UHF radar systems. This technique can be used to investigate neutral atmosphere variations as well as the validity of collision models commonly used in the IS formalism.

1. Introduction

The rate of collisions between ionized and neutral species is important for a variety of processes in the upper atmosphere. Collisions determine where field-aligned currents in the high-latitude ionosphere will close and thus where magnetospheric energy will be deposited [e.g., *Thayer*, 2000]. This energy is converted via Joule heating and Lorentz forcing, driving neutral motions, and heating of the neutral gas. Practically, collisions play a crucial role in deriving neutral winds, currents, Joule heating rates, and neutral atmospheric properties from measurements of ionized species, using techniques like incoherent scattering (IS).

Because the ion-neutral collision frequency (ν_{in}) depends largely on the neutral density (N_n), its measurement provides a direct linkage between the ionosphere and neutral atmosphere. However, there are very few methods to directly infer the neutral density or ν_{in} in the lower thermosphere, where the energy transfer rate maximizes. There are a limited number of practical ground-based techniques for sensing the lower thermosphere and the altitude regime is too low for routine in situ measurements.

Since the early 1960s, it has been recognized that ion-neutral collisions play an important role in IS measurements [*Dougherty and Farley*, 1963]. Collision frequency estimates have been reported for many years using the technique [e.g., *Wand and Perkins*, 1968; *Salah et al.*, 1975; *Wand*, 1976; *Tepley and Mathews*, 1978; *Schlegel et al.*, 1980; *Wickwar et al.*, 1981; *Lathuillere et al.*, 1983; *Fla et al.*, 1985; *Kofman et al.*, 1986; *Ganguly and Coco*, 1987; *Nygrén et al.*, 1987, 1989; *Huuskonen*, 1989; *Bjørnå*, 1989; *Reese et al.*, 1991; *Nygrén*, 1996; *Davies et al.*, 1997]. In most cases, ν_{in} is derived directly from fitting of the IS spectrum/autocorrelation function (ACF), which typically involves assumptions about ion and electron temperatures (often that they are equal and/or equal to the neutral temperature). *Bjørnå* [1989] used combined ion line and plasma line measurements to infer collision frequency profiles without any assumptions, using the measured plasma line resonance frequency at discrete heights in the IS fitting process. This is a viable technique when plasma lines can be detected in the *E* region. Another technique is to use the variation of measured ion drifts as a function of altitude [e.g., *Nygrén et al.*, 1987, 1989; *Davies et al.*, 1997; *Burchill et al.*, 2012]. The ions will transition from drifting with the neutral winds at low altitudes (collisional regime) to drifting at the $\mathbf{E} \times \mathbf{B}$ velocity at high altitudes (collisionless regime). This method typically involves assumptions about the neutral winds (often that they are negligible).

The assumptions required limit the utility of the IS measurements to static situations, when, for example, it might be justifiable to assume that $T_e = T_i (= T_n)$ where T_e, T_i, and T_n are the electron, ion, and neutral temperatures, respectively. This limitation precludes measurement in situations where the atmosphere is

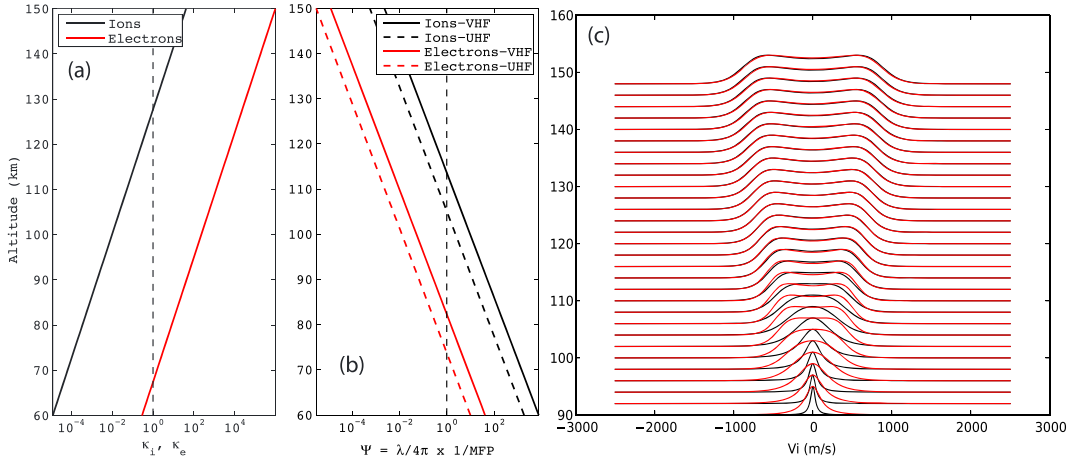

Figure 1. (a) κ_e and κ_i for the electrons and ions. (b) Characteristic correlation time for the electrons and ions for the European Incoherent Scatter (EISCAT) VHF and UHF systems. (c) Theoretical incoherent scatter ion line Doppler spectra (normalized) as a function of altitude for the EISCAT VHF (black) and EISCAT UHF (red) using realistic temperature, collision frequency, and electron density profiles (N_{mE} of 10^{11} m^{-3} at 115 km altitude, and temperatures from the Mass Spectrometer Incoherent Scatter (MSIS) model). The ionosphere is assumed to be composed purely of molecular species, and $T_e/T_i = 1$ at all altitudes.

most strongly affected, such as times of intense frictional and particle heating. As we show in this letter, multifrequency IS measurements can provide additional information on the collisionality of the medium [e.g., *Grassmann*, 1993b] and allow for the determination of ν_{in}, and thus neutral density, while minimizing the assumptions about the medium.

2. Multifrequency Incoherent Scatter Measurements

Figure 1a shows κ_e and κ_i, the ratio of the gyrofrequency to the collision frequency for the electrons and ions, respectively, as a function of altitude, using neutral densities from the NRLMSISE-00 empirical neutral atmosphere model [*Picone et al.*, 2002]. These quantities are important because they show where electrons and ions transition from collisionless to collisional electrodynamics. The ions are collisionless above ~130 km, whereas the electrons are collisionless at essentially all altitudes. This result underscores the utility of ion line IS measurements in the ionosphere: at high altitudes, ion motions are tracers for electric fields, whereas at low altitudes, they become tracers for neutral motions. More relevant to incoherent scattering is the collisionality of the plasma on the scale of the Bragg scattering wavelength. An ISR will be sensitive to collisions if the distance between collisions is $\ll \lambda/4\pi$ where λ is the probing wavelength. The particles then undergo a random walk with a characteristic correlation time given by the time it takes to travel a distance $\lambda/4\pi$.

To demonstrate the utility of multifrequency IS radar (ISR) measurements for studies of neutral properties in the lower thermosphere, we utilize the EISCAT Tromsø ISR systems (at 69.58°N,19.22°E), which include VHF (224 MHz) and UHF (933 MHz) transmitters. In addition, we collected data on two receive-only stations at VHF, located in Kiruna, Sweden, and Sodankylä, Finland. The characteristic correlation time is shown in Figure 1b for ions and electrons, for both the EISCAT VHF (224 MHz) and UHF (930 MHz) monostatic systems. The ion motion will transition between 100 and 120 km, and electrons undergo a transition between 70 and 90 km, with the exact region determined by the value of the electron and ion collision frequencies.

Data were collected on 19 August 2013 7–11 UT (local time ~ UT+1) as part of the EISCAT Peer-Review Program. System pointing and setup are shown in Table 1. Of critical importance for this study is the ability to measure IS spectra over a broad range of wave number (k) space. This need is enabled by the dual frequency, approximately common-volume UHF and VHF transmissions A. In addition, the bistatic links provide an additional independent measurement at a unique k, given by

$$k = |\mathbf{k}| = |\mathbf{k}_s - \mathbf{k}_i|$$

where $\mathbf{k}_s$ and $\mathbf{k}_i$ are the scattered and incident wave number vectors, respectively. For this particular experiment, the diversity in k provided by the bistatic links is not very significant, because of the particular

Table 1. System Parameters for the Tromsø (T) UHF and VHF Monostatic Systems, as Well as the Bistatic Kiruna (K) and Sodankylä (S) Links[a]

System	f (MHz)	λ (m)	k (rad/m)	Azimuth	Elevation	Range (Altitude) (km)
T (UHF)	933	0.32	39.0	0.0°	45.0°	49–694
T (VHF)	224	1.34	9.34	0.0°	45.0°	35–508
K (VHF)	224	1.34	9.08	351.0°	17.2°	312.8 (99.6)
S (VHF)	224	1.34	8.57	322.2°	9.8°	465.4 (95.3)

[a]Shown are the frequency, wavelength, wave number, azimuth, elevation, and range/altitude of detection.

geometry chosen. As a result of transmission constraints, the radars were required to be pointed vertically or to the north, which has the effect of making the incident and scattered wave numbers more parallel than they could be. For the remainder of this paper, we will focus on the monostatic measurements, but highlight the fact that bistatic links may provide the diversity in k necessary to realize these measurements. The 45° elevation angle for the Tromsø transmissions was chosen to mitigate clutter effects (particularly at VHF) and allow for measurements at the lags necessary to observe collisional effects. Both systems utilized a 640 μs, 20 μs (3 km) baud (32 bit) alternating code [*Lehtinen and Häggström*, 1987] sampled at 10 μs (1.5 km). IS autocorrelation functions were computed using 10 min averages prior to analysis.

Of most interest to this study are the differences in collisionality for the VHF and UHF probing wavelengths, which imply that ion line measurements in the 80–120 km altitude range will look differently when probed with different wavelengths. It was the purpose of this experiment to investigate those differences and demonstrate the utility of multifrequency ISR measurements for deriving information on the collisional

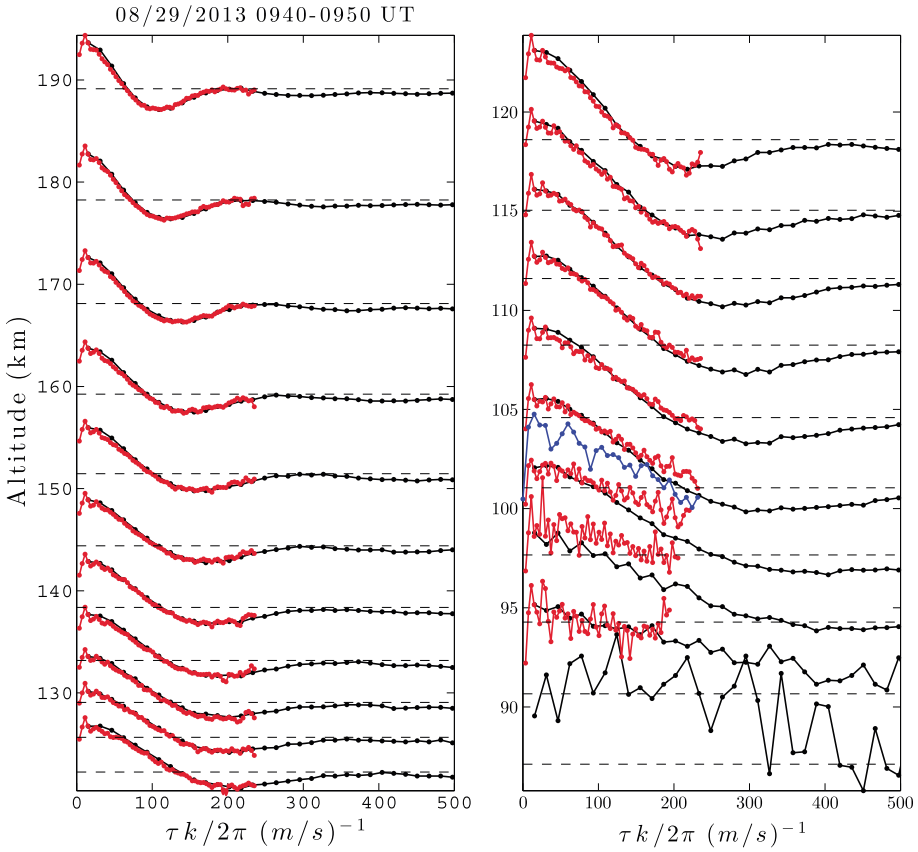

Figure 2. Measured autocorrelation functions as a function of altitude and normalized lag ($\tau k/2\pi$) for a single 10 min integration window on 29 August 2013. Measurements from the Tromsø UHF system are shown in black, from the Tromsø VHF in red, and from the Kiruna VHF in blue.

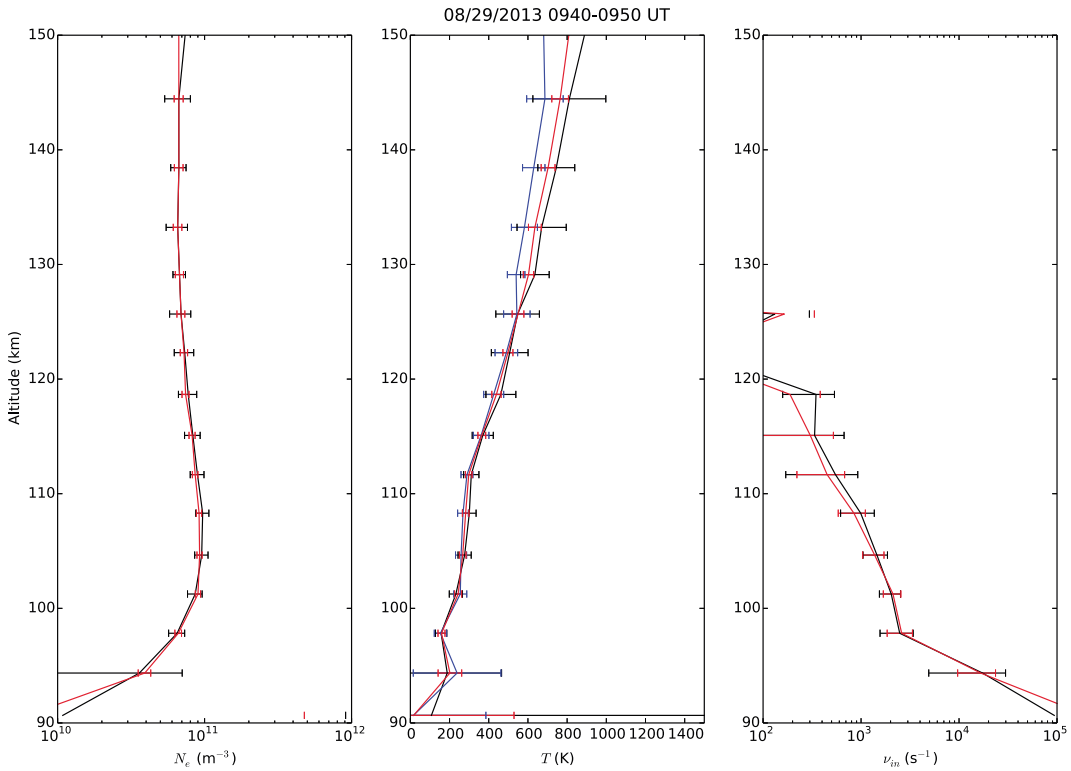

Figure 3. (left) N_e; (middle) T_e (black) and T_i (blue); and (right)ν_{in} for a single 10 min integration. Red curves show results constraining $T_e = T_i$, whereas blue and black curves allow $T_e \neq T_i$.

properties of the lower ionosphere. Example theoretical spectra are shown in Figure 1c that illustrate the change in the incoherent scatter spectrum as the ions pass through the collisional transition region. The VHF spectra will become sensitive to collisions at 110–120 km, and below that altitude strong differences exist in the Doppler spectra at the different wave numbers. Those differences should allow for a constrained IS fitting process to precisely derive ν_{in}.

Finally, in addition to these effects, in the lower ionosphere Debye-length shielding effects will reduce the absolute power received by the UHF system relative to the VHF system. Below densities of 10^{11}m^{-3}, the ratio of the power received at the two frequencies will deviate from unity and this provides information on T_e/T_i, which can be used to constrain inversions. At low densities and high-collision frequencies, the narrowing of the electron line causes increased power for a fixed bandwidth. To the extent that this information can be used to provide information on T_e/T_i, the composition, and other properties of the lower ionosphere can be investigated.

3. Results

Examples of autocorrelation function estimates from the VHF (red) and UHF (black) systems for a single 10 min integration window are shown in Figure 2. The lag axis has been normalized, and the ACFs are plotted as function of $\tau k/2\pi$ where τ is the lag time. Collisionless IS predicts the expected value of the normalized ACF (Fourier transform of the Doppler spectrum) to be identical. Indeed, this excellent agreement is evident from the higher altitude observations in Figure 2 (left). The ACFs as a function of normalized lag from the VHF and UHF are nearly identical. Below about 120 km, however, the correlation time of the VHF increases relative to that of the UHF. This is the expected observation due to the scale-dependent collisional effects. It is this feature of the measurements that allows for extraction of ν_{in}. The ACF from the Kiruna VHF bistatic measurements at 100–105 km shows a very similar effect.

A standard IS model was fit to the combined ACF measurements from the two different frequencies simultaneously using a nonlinear least squares fitting algorithm, with independent height-by-height fits (see also *Grassmann* [1993b]). Two different fitting approaches were employed. One used an assumption of $T_e = T_i$,

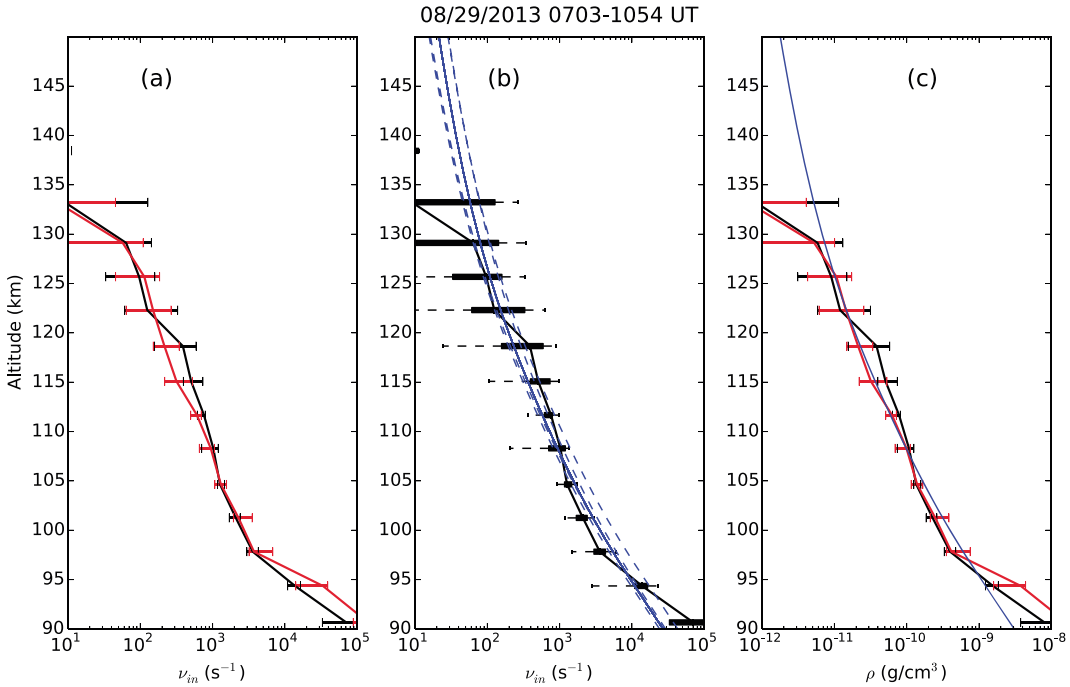

Figure 4. For the ~4 h integration window, (a) median ν_{in} using the constrained ($T_e = T_i$) fits (red), and the unconstrained fits ($T_e \neq T_i$) (black). Error bars span the interquartile range of the data. (b) ν_{in} for the unconstrained fits ($T_e \neq T_i$) (black). For each altitude, the box spans the interquartile range of the data. The dashed line out of each box shows the range of the data. The solid black line is at the median. The dashed blue lines correspond to MSIS collision frequencies for N_2^+, NO^+, O_2^+, and O^+, and the solid blue line is the composition-averaged collision frequency. (c) Estimated neutral mass density, ρ, for the median values using the method described in the text. The blue curve is the MSIS neutral density.

leaving free parameters N_e, ν_{in}, V_i, and T_i. A second fit relaxed that assumption to allow for fitting of both T_e and T_i. The standard density-conserving Bhatnagar-Gross-Krook (BGK) [*Bhatnagar et al.*, 1954] collision model was used [*Dougherty and Farley*, 1963; *Dougherty*, 1963]. A result for the 10 min integration window shown in Figure 2 is shown in Figure 3. Here we show N_e (left), T_e, T_i, and $T_e = T_i$ (middle), and ν_{in} (right). In this particular case, the $T_e = T_i$ assumption is valid up to ~125 km. Above that altitude, T_e begins to diverge from T_i and the constrained fit chooses a midpoint value for the temperature. For these observations, the effect of different temperatures on the collision frequency is not significant below 110 km. In the altitude range 110–120 km, the collision frequency estimates from the constrained fits ($T_e = T_i$) are somewhat lower than from the unconstrained fits ($T_e \neq T_i$), but these differences are within the error bars. Above ~125 km, the errors on ν_{in} are very large, the collision frequencies are small, and the methodology breaks down.

The estimates of ν_{in} below 120 km are extremely robust in terms of convergence properties and insensitivity to initial conditions. The collision frequencies decrease from $> 10^4 s^{-1}$ below 95 km to $< 10^3 s^{-1}$ at 120 km. These results demonstrate the utility of this approach, allowing for unconstrained ($T_e \neq T_i$) measurements of ν_{in} in the lower thermosphere with simultaneous determination of classical IS parameters (N_e, T_e, T_i, and V_i).

Averages of the collision frequency were computed over the 4 h observation window. These are shown in Figure 4a, for the constrained and unconstrained fits. Both show a nearly exponential decrease in altitude consistent with expectations. To show the full range of the data, the boxes in Figure 4b extend from the lower to upper quartile values of the constrained fits. The dashed line out of each box shows the range of the data. The solid black line is at the median. Overplotted are MSIS profiles in blue. MSIS collision frequencies were determined for each ion species, *i*, as

$$\nu_{in}^{MSIS} = \sum_n C_{in} N_n^{MSIS} \quad (1)$$

where N_n^{MSIS} is the number density for neutral species *n* obtained from MSIS, and C_{in} is either the nonresonant or resonant collision

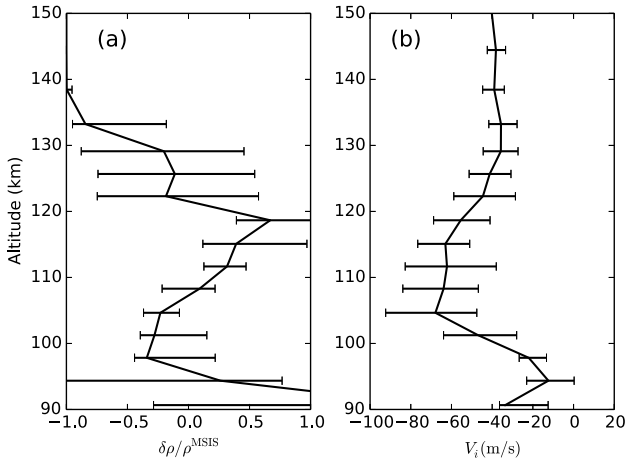

Figure 5. (a) Fractional deviation in ρ from MSIS and (b) line-of-sight ion velocity. Error bars span the interquartile range of the data over the 4 h integration window of Figure 4.

frequency coefficient (the latter being temperature dependent), obtained from *Schunk and Nagy* [2004]. The dashed blue lines in Figure 4 (middle) correspond to MSIS collision frequencies for N_2^+, NO^+, O_2^+, and O^+, and the solid blue line is the ion composition-averaged collision frequency. The MSIS values fall within the 25–75% values of the measurements at nearly all altitudes, with the exception of the 95–105 km range where the MSIS profiles are approximately 30–40% larger than the median value of the measurements. Shorter integration windows were investigated and these deviations persisted, implying statistical significance. The nature of the differences will be further investigated later.

Collision frequency can be converted to neutral density using a mass density model such that

$$\hat{\rho} = A\hat{\nu}_{\mathrm{in}} \tag{2}$$

where $\hat{\rho}$ is the total estimated mass density (the carat refers to an estimated quantity) and A is an altitude-dependent mass scaling factor, for which we use

$$A = \frac{\rho^{\mathrm{MSIS}}}{\sum_n C_{\mathrm{in}} N_n^{\mathrm{MSIS}}}. \tag{3}$$

(Note that this constraint enforces $\hat{\rho}/\hat{\nu}_{\mathrm{in}}$ = constant.) The mass density profiles are compared in Figure 4c.

Figure 5a shows the fractional deviation in the measured mass density from MSIS, with the error bars spanning the interquartile range of the 10 min estimates over the 4 h integration period. The fractional deviation from MSIS fluctuates around 0, indicating on average good agreement with MSIS. However, below ~110 km, the measured values are smaller than MSIS, by ~35%, and above ~110 km they deviate positively by a similar amount. The vertical half wavelength of this perturbation appears to be ~15 km. In Figure 5b, we plot the median line of sight ion velocity perturbation (close to the line-of-sight neutral wind at these altitudes) which shows a similar perturbation, but 90° out of phase. It thus seems possible that this perturbation is a result of a tide or low-frequency wave and not captured in the MSIS model.

4. Discussion and Conclusion

There are very few direct measurements of the collision frequency or neutral density in the lower thermosphere. Yet particle precipitation and Joule heating maximize in this region, affecting the density and thermal structure of the neutral and ion gases [e.g., *Schunk and Sojka*, 1995]. Molecular and turbulent diffusion are both important in this region, and the dynamics are also affected by tides, gravity waves, and other processes. The region is structured as a result of these phenomena.

Incoherent scatter measurements are sensitive to collisional properties of the ion gas in the mesosphere and lower thermosphere, where the mean free path is close to the radar wave number. This sensitivity provides a means to directly probe the neutral atmosphere in this region. Generally, however, it has been very difficult to infer these properties [e.g., *Huuskonen*, 1989] because of ambiguities in the theory for a measurement at a single wave number.

We have demonstrated that multifrequency measurements to achieve diversity in k can allow for direct inference of the composition-weighted ion-neutral collision frequency in the upper mesosphere and lower thermosphere, a technique first proposed by *Grassmann* [1993b]. By direct, we mean that no significant

constraints are imposed on the interpretation of the IS spectra and that the measurements rely only on the IS formalism (rather than a steady state ion-momentum equation, for example). We have demonstrated the technique using measurements from the EISCAT VHF and UHF radar systems in Tromsø, Norway. Over a 4 h, quiet, daytime observation window, median values agree with MSIS-predicted values to within ~40%. The deviation from MSIS oscillates with altitude with a vertical wavelength of ~30 km, correlated but out of phase with the ion velocity, which we hypothesize to be due to a tidal or low-frequency wave perturbation. This technique provides a direct measure of the neutral density and can be used to investigate neutral atmosphere variations, for example, associated with magnetospheric energy input and lower atmospheric forcing.

Moreover, IS inferences of other parameters, such as the neutral wind fields, are often based off of a steady state ion-momentum equation and rely on a model for the neutral atmosphere [e.g., *Heinselman and Nicolls*, 2008]. A direct measurement of the collision frequency eliminates the need to use a model atmosphere in these calculations. In addition, the nature of the collision operator in IS theory has always been somewhat ad hoc. Most approaches, including this study, use a BGK collision operator that conserves particle density [*Dougherty*, 1963]. However, other approaches, such as a BGK approach that conserves density, momentum, and energy and Fokker-Planck operators [e.g., *Hagfors and Brockelman*, 1971] may be more valid, and indeed may produce significantly different results [e.g., *Grassmann*, 1993a]. Direct measurements of the IS spectrum at significantly different frequencies provide a means to test these theories.

Acknowledgments

M.J.N. and H.B. appreciate the radar time afforded by the EISCAT Peer-Review Program that enabled these measurements. EISCAT is an international association supported by research organizations in China (CRIRP), Finland (SA), Japan (NIPR and STEL), Norway (NFR), Sweden (VR), and the United Kingdom (NERC). EISCAT data used in this paper are available for download through the EISCAT schedule webpage (http://www.eiscat.se/schedule/). Research at SRI International was supported by NSF Cooperative Agreement AGS-1133009 and NSF grant AGS-1139152. M.J.N. acknowledges useful discussions with Craig Heinselman, Director of the EISCAT Scientific Association.

W.K. Peterson thanks Mike Kosch and one anonymous reviewer for their assistance in evaluating paper.

References

Bhatnagar, P. L., E. P. Gross, and M. Krook (1954), A model for collision processes in gases. I. Small amplitude processes in charged and neutral one-component systems, *Phys. Rev.*, *94*, 511–525, doi:10.1103/PhysRev.94.511.

Bjørnå, N (1989), Derivation of ion-neutral collision frequencies from a combined ion line/plasma line incoherent scatter experiment, *J. Geophys. Res.*, *94*(A4), 3799–3804.

Burchill, J. K., J. H. Clemmons, D. J. Knudsen, M. Larsen, M. J. Nicolls, R. F. Pfaff, D. Rowland, and L. Sangalli (2012), High-latitude E region ionosphere-thermosphere coupling: A comparative study using in situ and incoherent scatter radar observations, *J. Geophys. Res.*, *117*, A02301, doi:10.1029/2011JA017175.

Davies, J. A., M. Lester, and T. R. Robinson (1997), Deriving the normalised ion-neutral collision frequency from EISCAT observations, *Ann. Geophys.*, *15*, 1557–1569.

Dougherty, J. P. (1963), The conductivity of a partially ionized gas in alternating electric fields, *J. Fluid Mech.*, *16*, 126–137.

Dougherty, J. P., and D. T. Farley (1963), A theory of incoherent scattering of radio waves by a plasma: 3. Scattering in a partly ionized gas, *J. Geophys. Res.*, *68*(19), 5473–5485.

Fla, T., S. Kirkwood, and K. Schlegel (1985), Collision frequency measurements in the high-latitude *E* region with EISCAT, *Radio Sci.*, *20*(4), 785–793.

Ganguly, S., and D. Coco (1987), Incoherent scattering from the collision dominated *D*-region: Comparison of theories with experimental data, *J. Atmos. Terr. Phys.*, *49*(6), 549–563.

Grassmann, V. (1993a), The effect of different collision operators on EISCAT's standard data analysis model, *J. Atmos. Terr. Phys.*, *55*, 567–571.

Grassmann, V. (1993b), An incoherent scatter experiment for the measurement of particle collisions, *J. Atmos. Terr. Phys.*, *55*, 573–576.

Hagfors, T., and R. A. Brockelman (1971), A theory of collision dominated electron density fluctuations in a plasma with applications to incoherent scattering, *Phys. Fluids*, *14*, 1143, doi:10.1063/1.1693578.

Heinselman, C. J., and M. J. Nicolls (2008), A Bayesian approach to electric field and *E*-region neutral wind estimation with the Poker Flat Advanced Modular Incoherent Scatter Radar, *Radio Sci.*, *43*, RS5013, doi:10.1029/2007RS003805.

Huuskonen, A. (1989), High-resolution observations of the collision frequency and temperatures with the EISCAT UHF radar, *Planet. Space Sci.*, *37*, 211–221.

Kofman, W., C. Lathuillere, and B. Pibaret (1986), Neutral atmosphere studies in the altitude range 90–110 km using EISCAT, *J. Atmos. Terr. Phys.*, *48*, 837–847.

Lathuillere, C., V. B. Wickwar, and W. Kofman (1983), Incoherent scatter measurements of ion-neutral collision frequencies and temperatures in the lower thermosphere of the auroral region, *J. Geophys. Res.*, *88*(A12), 10,137–10,144.

Lehtinen, M. S., and I. Häggström (1987), A new modulation principle for incoherent scatter measurements, *Radio Sci.*, *22*, 625–634, doi:10.1029/RS022i004p00625.

Nygrén, T. (1996), Studies of the E-region ion-neutral collision frequency using the EISCAT incoherent scatter radar, *Adv. Space Res.*, *18*(3), 79–82.

Nygrén, T., L. Jalonen, and A. Huuskonen (1987), A new method of measuring the ion-neutral collision frequency using incoherent scatter radar, *Planet. Space Sci.*, *35*(3), 337–343.

Nygrén, T., B. S. Lanchester, L. Jalonen, and A. Huuskonen (1989), A method for determining the ion-neutral collision frequency using radar measurements of ion velocity in two directions, *Planet. Space Sci.*, *37*, 493–502.

Picone, J. M., A. E. Hedin, D. P. Drob, and A. C. Aikin (2002), NRLMSISE-00 empirical model of the atmosphere: Statistical comparisons and scientific issues, *J. Geophys. Res.*, *107*(A12), 1468, doi:10.1029/2002JA009430.

Reese, K. W., R. M. Johnson, and T. L. Killeen (1991), Lower thermospheric neutral densities determined from Sondre Stromfjord incoherent scatter radar during LTCS 1, *J. Geophys. Res.*, *96*(A2), 1091–1098.

Salah, J. E., J. V. Evans, and R. H. Wand (1975), *E*-region measurements at Millstone Hill, *J. Atmos. Terr. Phys.*, *37*, 461–489.

Schlegel, K., H. Kohl, and K. Rinnert (1980), Temperatures and collision frequency in the polar *E* region, *J. Geophys. Res.*, *85*(A2), 710–714.

Schunk, R. W., and A. Nagy (2004), *Ionospheres: Physics, Plasma Physics, and Chemistry*, Cambridge Univ. Press, Cambridge.

Schunk, R. W., and J. J. Sojka (1995), The lower ionosphere at high latitudes, in *The Upper Mesosphere and Lower Thermosphere: A Review of Experiment and Theory*, pp. 37–47, AGU, Washington, D. C., doi:10.1029/GM087p0037.

Tepley, C. A., and J. D. Mathews (1978), Preliminary measurements of ion-neutral collision frequencies and mean temperatures in the Arecibo 80- to 100-km altitude region, *J. Geophys. Res.*, *83*(A7), 3299–3302.

Thayer, J. P. (2000), High-latitude currents and their energy exchange with the ionosphere-thermosphere system, *J. Geophys. Res.*, *105*(A10), 23,015–23,024.

Wand, R. H. (1976), Semidiurnal tide in the *E* region from incoherent scatter measurements at Arecibo, *Radio Sci.*, *11*(7), 641–652.

Wand, R. H., and F. W. Perkins (1968), Radar Thomson scatter observations of temperature and ion-neutral collision frequency in the *E* region, *J. Geophys. Res.*, *73*(19), 6370–6372.

Wickwar, V. B., C. Lathuillere, W. Kofman, and G. Lejeune (1981), Elevated electron temperatures in the auroral *E* layer measured with the Chatanika radar, *J. Geophys. Res.*, *86*(A6), 4721–4730.